Transactions on Modelling and Simulation vol 10, © 1995 WIT Press, www.witpress.com, ISSN 1743-355X

Wavelet analysis of near wall turbulent boundary layer velocity signal

G. Iuso,[a] M. Onorato Jr[b]

[a] *Dipartimento di Ingegneria Aeronautica, Politecnico di Torino, Corso Duca Degli Abruzzi, 24-10029 Torino, Italy*

[b] *Istituto di Fisica Generale, Università di Torino, Via Pietro Giuria, 1-10125 Torino, Italy*

Abstract

Classical eduction schemes for turbulent boundary layer bursting processes are based on the assumption of empirical threshold constants. The wavelet analysis has been recently considered to be a possible candidate as turbulent structure detection method, overcoming any empirical approach.
An application of this mathematical tool to a near wall boundary layer velocity signal is shown. Comparison with classical VITA detection scheme is presented.

1 Introduction

It is well known that turbulence production in turbulent boundary layers is a quasi-periodic process which results in energetic production of turbulent energy termed 'bursting'. A detailed understanding of the bursting process is of great importance both for dynamic modelling of the turbulence production mechanisms and for developing methods to control skin friction drag and wall heat transfer. For this reason, after the pioneer studies of Kline, Reynolds, Schraub and Runstadler (1967) at Stanford University [1] and Corino and Brodkey (1969) at Ohio State University [2], a great amount of work has been

done on the subject. These studies rely heavily on flow visualization and hot wire measurements and on a combination of the two techniques. A comprehensive review of the past and recent studies is given in the paper of Robinson (1991) [3].

A large contribution to the understanding of the bursting process has been recently given by complete numerical simulation of boundary layer flows [4] and fully developed turbulent channel flows [5]. It has become increasingly clear that the underlying mechanisms of turbulent energy (and Reynolds stress) production are inextricably linked to the dynamics of organized coherent vortical structures in the wall region. These structures appear in a variety of repetitive forms and at different scales and levels of activity. More recently Bernard et al. [6], by analysing a numerically simulated channel flow at Re=125 based on velocity friction and channel half width, reconstructed the near wall vortical events suggesting a complete scenario by which vortices evolve in the turbulent boundary layer, showing capacity for self-replication and leading to a continual supply of new structures. In this scenario, the interaction of counter-rotating pairs of vortices appears to be the cause of the observed bursting process, consisting on ejection and inrush of fluid particles, events that are responsible of the turbulent energy production.

In spite of the considerable amount of information obtainable by the complete numerical simulation, the results are restricted to simple flow configuration and to very low Reynolds numbers, far from most of practical applications.

The experimental approach is still of great importance to study the dynamical role of the vortices in producing turbulent energy. Unlikely, in ordinary turbulent flows, the coherent structures are embedded inside the overall chaotic behaviour of the turbulence field and are then very difficult to detect. Moreover the three dimensional nature of the structure makes their eduction a very complex task, especially for single-point measurements.

Several techniques for detecting bursting events have been developed during the past twenty years. Each of these detection algorithms is based on a velocity-signal pattern that is postulated to be a unique characteristics of the bursting events. These techniques were based on the local variance of the streamwise u -velocity component [7,8], on the local value of the u -velocity [9] or on its slope [10], on the sign of the uv product [9], were v is the velocity component

normal to the wall. All these detection algorithms rely on the assumption of a threshold, whose value is empirically established, mostly by correlation with flow visualization results.

The aim of this paper is to show an application of a new developing technique, the wavelet transform analysis, as a structure eduction method for turbulence flow, that overcome any empirical approach.

Results obtained with this technique will be compared with results obtained with the classical variable interval time averaged method (VITA).

2. Wavelet Transform

The most used tool for analysing time series is certainly the Fourier Transform. This method allows to decompose a signal, or more generally a function in L^2 as a superposition of sinusoidal waves. Unfortunately these oscillate from $-\infty$ to ∞, and cannot adequately describe the behaviour of the signal at a specific time. If we consider as an example, a function $f(x)$ which is smooth everywhere except for a singularity, and if we take a FFT, we will end up with a power law spectrum that tells us that the function is globally non regular: we lost the essential information, that is, $f(x)$ has a local singularity. Wavelet transform [11,12] provides an alternative way for analysing signals: the trigonometric functions of the Fourier Transform are now replaced by other functions, called *wavelets,* which are localized in physical space. The signal can then be written as a linear superposition of wavelets at different *position* and *scale* and the coefficients of the expansion give information on the local behaviour of the signal. Starting from a single analysing function $g(t)$, we construct by translation and dilatation:

$$g_{a,t_0}(t) = p(a)g\left(\frac{t-t_0}{a}\right), \tag{2.1}$$

where a is the scale and $p(a)$ is a weighting function. The wavelet transform of a signal $f(t)$ is defined as

$$T_g(a,t_0) = p(a)\int_{-\infty}^{\infty} f(t)g\left(\frac{t-t_0}{a}\right)dt \tag{2.2}$$

In order to perform a wavelet transform it is necessary that the function $g(t)$ satisfies a number of conditions: it must have a zero mean (admissibility condition) and it must be localised in physical and in Fourier space. Different weighting functions can be used. If $p(a) = a^{-1/2}$, [13], then each element of the family of a wavelet contains the same energy, so that the square modulus of the coefficients of the expansion, $|T_g(a,t_0)|^2$, known as the *local* wavelet energy spectrum, gives information about the distribution of energy at different scales and positions. Another common choice for the weighting function is $p(a) = a^{-1}$ [14], [15] which has the effect of intensifying the small scales.Therefore the role of the weighting function is to accentuate or suppress the desired scales of the decomposition. Since we look for localized energetic structures, we will adopt the first choice, $p(a) = a^{-1/2}$.

The scale a is related to the wave number k in the following way: $k = c / a$; the constant c depends on the family of wavelet. For the Mexican hat, which analytical form is given by the second derivative of a gaussian function (Fig.1), c is found to be equal to $\sqrt{2}$ [16].

The wavelet transform is also invertible, the reconstruction formula for the case of $p(a) = a^{-1/2}$ has the following form:

$$f(t) = \frac{1}{C_g}\int_0^\infty \frac{da}{a^2}\int_{-\infty}^{\infty} T_g(a,t_0)\frac{1}{a^{1/2}}g\left(\frac{t-t_0}{a}\right)dt_0 \tag{2.3}$$

where

$$C_g = \int_0^\infty \frac{|\hat{g}(k)|^2}{k}dk, \tag{2.4}$$

with $\hat{g}(k)$ being the Fourier Transform of $g(t)$.

It can be shown [17] that for Mexican hat the inverse transform formula simplifies to become

$$f(t) = C\int_0^\infty a^{1/2}T_g(a,t_0)\frac{da}{a^2} \tag{2.5}$$

The exact value of the C is given in reference [17]. For the wavelet transform the Parseval's theorem holds:

$$\int_{-\infty}^{\infty} |f(t)|^2 dt = \frac{1}{C_g} \int_{-\infty}^{\infty} |T_g(a,t_0)|^2 \frac{da dt_0}{a^2} \tag{2.6}$$

The energy distribution among all scales (wavelet power spectrum) is given by

$$E(a) = \frac{1}{C_g} \int_{-\infty}^{\infty} |T_g(a,t_0)|^2 \frac{dt_0}{a^2} \tag{2.7}$$

It is also possible to evaluate the distribution of energy as a function of time (*local* energy density):

$$E(t_0) = \frac{1}{C_g} \int_{-\infty}^{\infty} |T_g(a,t_0)|^2 \frac{da}{a^2} \tag{2.8}$$

3. VITA Detection Scheme

The VITA technique, devised by Blackwelder and Kaplan [7] is based on the intermittent character of the short-time variance of a turbulent signal. This quantity gives a local measure of the turbulent activity. The short-time variance of a signal $u(t)$ is defined as

$$\mathrm{var}_u(t,T) = \frac{1}{T} \int_{t-\frac{T}{2}}^{t+\frac{T}{2}} [u(s)]^2 ds - \left(\frac{1}{T} \int_{t-\frac{T}{2}}^{t+\frac{T}{2}} u(s) ds \right)^2 \tag{3.1}$$

where T is the short time averaging time.

An event is considered to occur when the variance exceeds ku_{rms}^2, where k is a chosen threshold level and

$$u_{rms}^2 = \lim_{T \to \infty} \mathrm{var}_u(t,T) \tag{3.2}$$

A detection function D(t) is defined as

$$D(t) = \begin{cases} 1 \text{ if } \mathrm{var}_u(t,T) > k u_{\mathrm{rms}}^2 \\ 0 \qquad \text{otherwise} \end{cases} \tag{3.3}$$

Once a reference time for each burst has been determined by the detection function, it is possible to study the bursting phenomenon by using conditional averaging techniques:

$$< u(\tau) > = \frac{1}{N} \sum_{j=1}^{N} u(t_j + \tau) \tag{3.4}$$

where the quantities t_j are the reference times, taken as the midpoints of the events, N is the number of events and τ is a time coordinate relative to a reference time t_j.

In this paper the VITA technique is simply used as a bursting detection scheme, assuming a threshold level of $k = 1$.

4. Experimental Considerations

The experiments were performed on a splitter plate mounted horizontally in the test section of the 0.70m x 0.50m low speed, open circuit, wind tunnel of the "Politecnico di Torino". The pressure gradient along the plate was nearly zero. The transition from laminar to turbulent flow was fixed at the splitter plate leading edge. The data here analysed were taken at a distance from the leading edge of 1260mm and at an height from the plate of 20 wall characteristic lengths, $y^+ = y u_t / \nu = 20$. This position corresponds to the buffer layer region, where the maximum production of turbulent energy is expected. The Reynolds number ($Re = u_t \theta / \nu$, where θ is the momentum thickness) at the measurement point was Re=125; the ratio between the friction velocity u_t and the external velocity was 0.04.

Single normal hot wire probe was used for the u -component of the fluctuating velocity measurements, using a constant temperature Dantec System. The a. c. part of the hot wire signal, amplified, was acquired by a 12

bit analog-to-digital converter, at 6 khz sampling rate. The accuracy of the measurements may be evaluated as less than 2%. The ratio between the r.m.s. value of the fluctuating velocity and the external velocity was 0.06.

5. Results and Comments

In order to illustrate the variety of information that may be obtained by the wavelet analysis, grey level plot of the wavelet coefficients $T_g(\lambda,t_0)$, where $\lambda = 1/a$, are shown in Figure 2. The duration λ and the time t_0 have been normalised respect to the wall characteristic time ν/u_τ^2. Regions where $T_g(\lambda,t_0)$ are large indicate high correlation between the data and the wavelet. It is evident the intermittent nature of the data, where positive and negative values of the wavelet coefficient show a quasi-alternate behaviour. Peaks with negative values of $T_g(\lambda,t_0)$ corresponds to events where the fluctuating u -velocity shows preferably positive values and positive peaks correspond to wall activities where the u -velocity tends to be negative. Finally it is evident in the large amount of scales involved in the phenomenon.

The wavelet power spectrum and its equivalent Fourier power spectrum are shown in Fig.3. The two spectra have been normalized with respect to the values of the area under the curves. The scales of the y-axis are arbitrary. The wavelet method seems to give a smoother representation of the spectrum, as it was already observed in Ref. [18] for boundary layer velocity signals over the ocean. A direct comparison between wavelet and VITA analysis is shown in Figure 4 and 5, for a set of data including 500 sample points, corresponding to 0.08 seconds. The time distribution of the energy integrated over all scales, $E(t)$, obtained by equation (2.8), is shown in comparison with the VITA detection function. The y-scale is arbitrary. The VITA detection function in Figures 4 and 5 has been evaluated using two different values of the short non dimensional averaging time, respectively $T^+ = 10$ in Fig. 4 and $T^+ = 20$ in Fig. 5. It may be observed that events detected with VITA correspond rather well with instants in which $E(t)$ assumes peak values. Similar results have been obtained by Benaissa et al. [19]. Looking in detail, one of the higher $E(t)$ peak in Fig. 4, at $t^+ = 420$, is not detected by VITA method at $T^+ = 10$ and conversely is detected at higher averaging time, Fig. 5. It should be noticed that the VITA variance is strongly dependent on the value of averaging time

window, T^+, which acts as a filter in the velocity data. Therefore VITA has the tendency to detect events occurring in a scale comparable with T^+. Going further in details, it may be seen that events corresponding to smaller scales, detected at about $t^+ = 1365$ and $t^+ = 1440$ for $T^+ = 10$ (Fig. 4), are not revealed in the case of $T^+ = 20$ (Fig. 5).

Two subsets of the previous results are shown in Figures 6 and 7; the velocity signal is also reported. In order to make a categorisation of the observed events, attention must be put on the slope of the velocity signal at the detection time. As it is clearly shown in the velocity sequence,Figures 6 and 7, events are characterised by either a slow velocity deceleration followed by a sharp acceleration (accelerated event), or a slow acceleration followed by a sharp deceleration (decelerated event). This categorization is in line with the observations in Ref. [20] using hydrogen-bubble visualization-derived data. As it is reported in Ref. [20], the accelerated event is the one most commonly accepted time burst-type event, characterized as an ejection of low-momentum fluid from the surface, followed by a rapid acceleration or "sweep" of high-momentum fluid. The decelerated events seem to reverse this process and in most studies they are discounted when attempting to establish "bursting" times, retaining only the accelerated events.

From the present results, it may be argued that during the decelerated events, amount of turbulent energy as large as for the accelerated events are involved, even if the frequency of decelerated events appear to be much lower. Moreover, referring to the scenario from direct numerical simulation, counter-rotating pairs of vortices may promote both ejection and inrush of fluid particles. The latter may explain decelerated events. Beside the single detection events described, we may expect also sequential and parallel events. The former, detectable by point measurements, may be defined as events occurring temporally close, $\Delta t^+ < 20$, in probe region. They may have the feature of accelerated or decelerated events or both. According to this categorization, the two aligned events in Fig. 6, near the origin, that are separated by an interval of time of about $\Delta t^+ = 19$, may be grouped in only one bursting process and considered as a multiple type event. Parallel events are supposed to occur at about the same time, but at different heights above the plate surface. Clearly only one event may be detected by point measurements, but it is clear also that the influence of

the parallel event may be present in the probe region, appearing as energy or scale magnification.

Because of the three-dimensional complexity of scales that are associated with turbulent boundary layers, an appropriate burst detection approach must be able to observe variations in scales of both length and time. The former can not be accomplished by point measurements; particle image velocimetry may be a good candidate for this task in competition with direct numerical simulations. For the latter, a contribution may come from the wavelet analysis. In Fig. 8 contour plot of energy are shown as a function of scale and time. Looking at the iso-lines, regions of concentrated turbulent energy are observed in correspondence of the time in which bursting activities have been detected, as reported in Figures. 4 and 5, retaining information about the scales. The results shown in Fig. 8 appear to be promising for a statistical approach of the scale problem, leading to the probability distribution of events respect to scales. A possible statistical analysis may take also into account the characterisation of the events, distinguishing between decelerated and accelerated events.

6. Conclusions

A near wall turbulent boundary layer fluctuating velocity signal has been analysed using wavelet transform. It has been confirmed that the wavelet power spectrum gives a smoother representation respect to the equivalent Fourier power spectrum. Comparisons between the local wavelet energy density distribution eduction method and the VITA detection function are in good agreement, provided that the VITA short averaging time T^+ window is properly chosen, according to the scale of the events.

In line with the observations in Ref. [20], the events have been characterised and interpreted as accelerated events and decelerated events.

A proper statistical approach is under study in order to take into account the information present in the local wavelet energy spectrum, where events appear to spread in a wide range of scales.

Acknowledgements: This research was sponsored by the National Ministry of Education under MPI 60% program and by the Centro Studi sulla Dinamica dei Fluidi del C.N.R.

References

1. Kline, S.J., Reynolds, W.C., Schraub, F.A. & Runstadler, P.W. The structure of turbulent boundary layers, *J. Fluid Mech.*, 1967, **95**.

2. Corino, E.R. & Brodkey, R. S., A visual investigation of the wall region in turbulent flow, *J;. Fluid Mech.*, 1969, **37**.

3. Robinson, S.K. Coherent motion in the turbulent boundary layer, *Annu. Rev. Fluid Mech.*, 1991, **23**, 601-639.

4. Robinson, S. K., Kline, S. J. & Spalart, P. R. Quasi-coherent structures in the turbulent boundary layer: part II verification and new information from a numerically simulated flat-plate layer, (ed. S. J. Kline, Hemisphere), *Proceedings Zaric Int. Seminar on Wall Turbulence*, 1989.

5. Kim, J., Moin, P. & Moser, R. Turbulence statistics in fully developed channel flow at low Reynolds number, *J. Fluid Mech.*, 1987, **177**.

6. Bernard,.P. S., Thomas, J.T. & Handler, R.A..Vortex dynamics and the production of Reynolds stress, *J. Fluid Mech.*, 1993, **253**, 385-419.

7. Blackwelder, R. F. & Kaplan, R. E. On the bursting phenomenon near the wall in bounded turbulent shear flows, *J. Fluid Mech.*, 1976, **76**.

8. Blackwelder, R. F. & Haritonidis, J. H. Scaling of the burst frequency in turbulent boundary layers *J. Fluid Mech.*, 1983, **132**.

9. Lu, S. S. & Willmarth, W. W. Measurement of structure of the Reynolds stress in a turbulent boundary layer, 1973, **60**.

10. Chen, C. P. & Blackwelder, R. F. The large-scale motion in a turbulent boundary layer: a study using temperature contamination, *J. Fluid Mech.*, 1987, **89**.

11. Grossman, A. & Morlet, J. *Mathematics and Physics, Lectures on Recent Results* (ed. L. Streit) , World Scientific, Singapore, 1987.

12. Farge, M. Wavelet transforms and their applications to turbulence, *Annu. Rev. Fluid Mech.*, 1992, **24**, 395-457.

13. Liandrat, J. & Moret-Bailly, F. The wavelet transform: some applications to fluid dynamics and turbulence, *Eur. J. Mech. B/Fluids*, 1990, **9**, 1-19.

14. Holschneider, M. On the wavelet transformation of fractal object, *J. Stat. Phys.*, 1988, **50**, 963-993.

15. Bacry, E. *Wavelet analysis of fully developed turbulence data and measurement of scaling exponents.* Turbulence and Coherent Structures (eds O. Méteis & M. Lesieur), Kluwer Academic Publisher, 1991.

16. Onorato, M.jr Analisi di moti ondosi nel Mare Adriatico, *Tesi di Laurea*, 1994, Università degli Studi di Torino.

17. Lewalle, J. Wavelet transforms of some equations of fluid mechanics, to appear in Acta Mech., 1994.

18. Meyers, S.D., Kelly, B.J., O'Brien J.J. An Introduction to Wavelet Analysis in Oceanography and Meteorology: with application to the dispersion Yanai Waves, *Monthly Weather Review,* 1991, **121**.

19. Benaissa, A., Anselmet, F., Moret-Bailly, F. & Liandrat, J., *In Eddy Structure Identification in Free Turbulent Shear Flows*, Kluwer Acad. Publ., 1993.

20. Lu, L. J. & Smith, C. R. Use of flow visualization data to examine spatial-temporal velocity and burst-type characteristics in a turbulent boundary layer, *J. Fluid Mech.*, 1991, **232**.

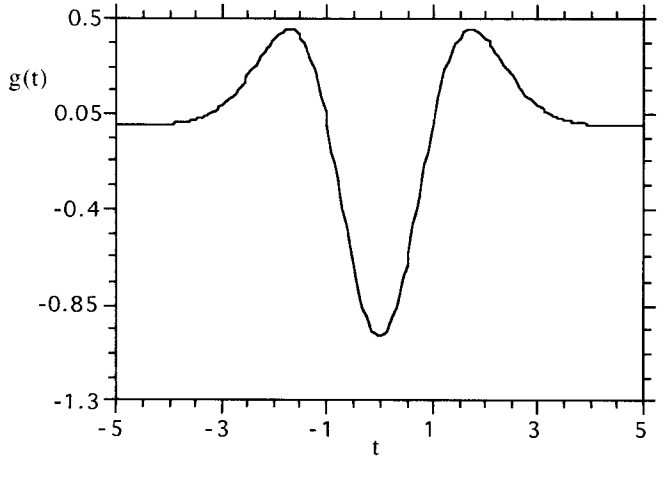

Figure 1: Mexican hat wavelet

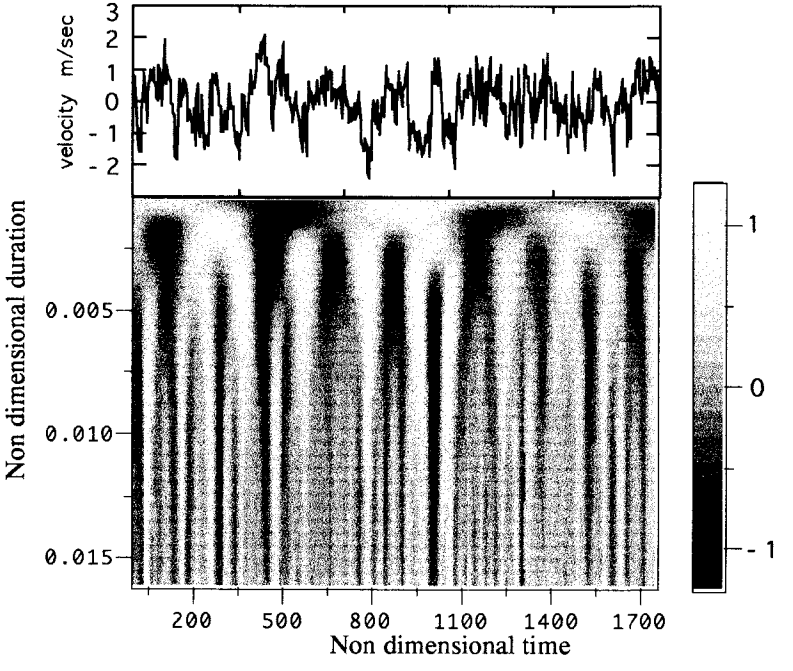

Figure 2: Grey level plot of the wavelet coefficients and the respective time serie.

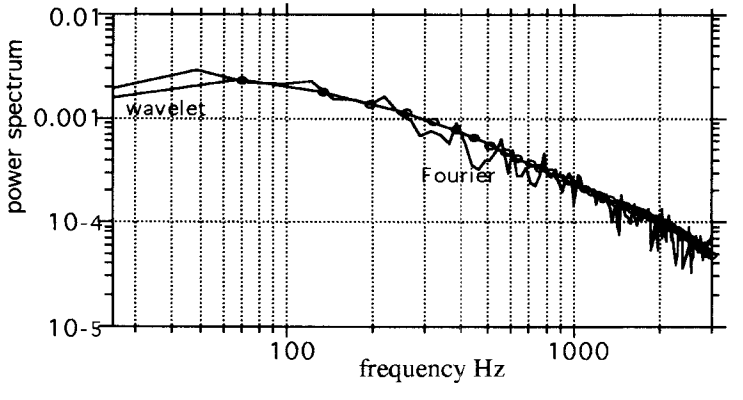

Figure 3: Wavelet and Fourier power spectra

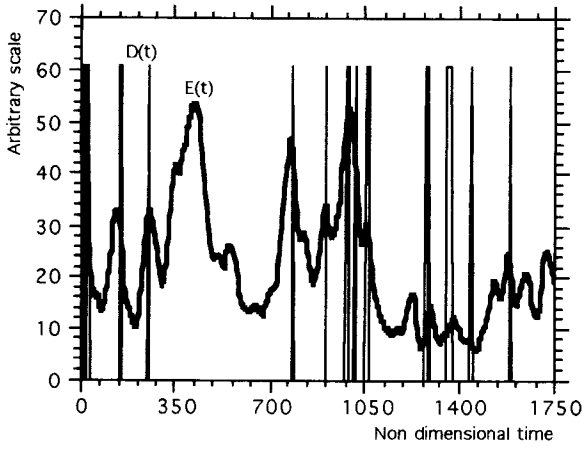

Figure 4: Comparison between wavelet local energy density E(t) and VITA detection function D(t), with $k=1$, $T^{+} = 10$

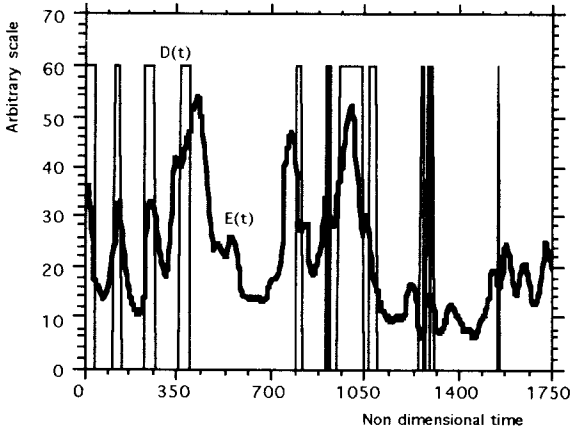

Figure 5: Comparison between wavelet local energy density E(t) and VITA detection function D(t), with $k=1$, $T^{+} = 20$

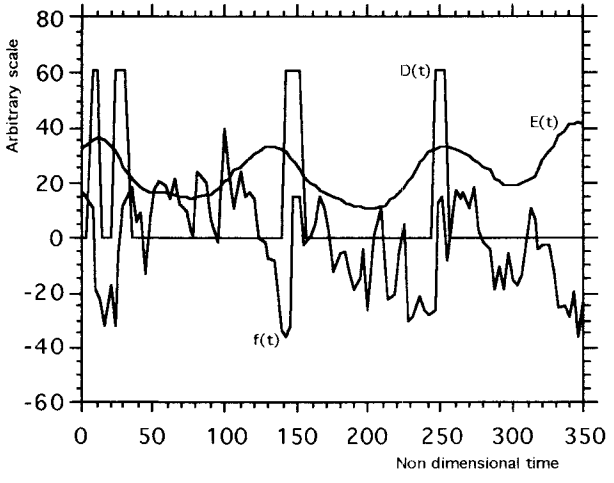

Figure 6: Wavelet local energy density E(t), VITA detection function D(t), with $k=1$, T^{+} = 10 and u -signal f(t).

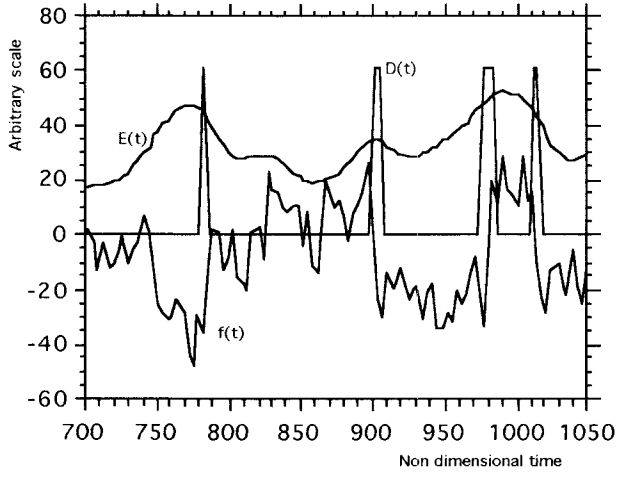

Figure 7: Wavelet local energy density E(t), VITA detection function D(t), with $k=1$, T^{+} = 10 and u -signal f(t).

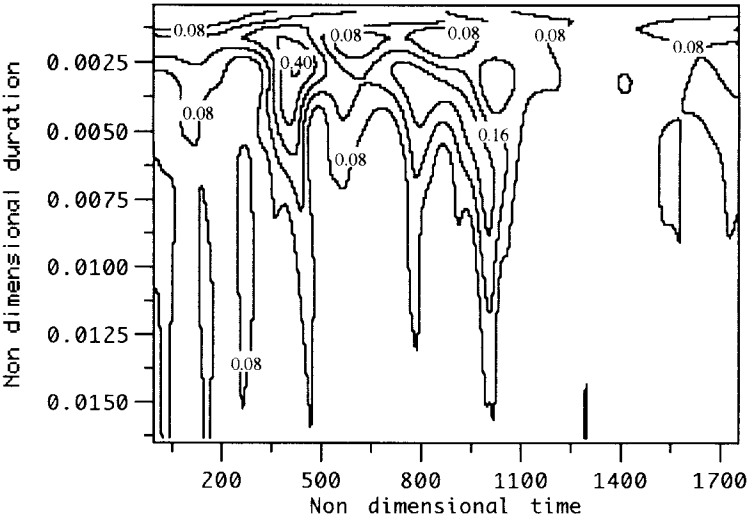

Figure 8: Contour plot of the local wavelet energy spectrum $|T_g(\lambda, t_0)|^2$